

## Evidence for nonlinear screening and enhancement of scattering by a single Coulomb impurity for dielectrically confined electrons in InAs nanowires

J. Salfi,<sup>\*</sup> S. V. Nair, I. G. Savelyev, M. Blumin, and H. E. Ruda

*Centre for Nanotechnology, University of Toronto, 170 College Street, Toronto, Ontario, Canada M5S 3E4*

(Received 7 December 2011; revised manuscript received 22 May 2012; published 22 June 2012)

The conductance due to scattering by a single repulsive Coulomb impurity is measured as a function of gate voltage in backgated InAs nanowires by analysis of random telegraph noise. Comparison with a quantum mechanical theory for carrier response and scattering reveals that the large dielectric mismatch between the nanowire and its surroundings enhances the Coulomb interaction, produces a nonlinear screening process that weakens dielectric response, and enhances the self-consistent Coulomb-impurity barrier of a single repulsive impurity, as nanowire diameter is reduced. Consequently, the scattering rate by such an impurity is enhanced by nearly two orders magnitude for 30 nm diameter InAs nanowires. A dramatic asymmetry of scattering by repulsive and attractive impurities, where the latter produce majority carriers, explain how a single repulsive impurity can control the conductance of a 1  $\mu\text{m}$  long InAs nanowire. Relevance to proposed nanoelectronic and sensing devices is discussed.

DOI: [10.1103/PhysRevB.85.235316](https://doi.org/10.1103/PhysRevB.85.235316)

PACS number(s): 73.63.Nm

The many-body dielectric response (screening) by carriers experiencing confinement in nanostructures depends on carriers' mutual interactions and electronic structure, and therefore differs from that of bulk systems. In quasi-one-dimensional (Q1D) electronic systems, with geometrically the fewest degrees of freedom to screen perturbations, it is a topic of continued theoretical investigation.<sup>1-9</sup> Semiconductor nanowires (NWs) have recently emerged as model systems for studying Q1D electronic phenomena,<sup>10-12</sup> but the dielectric response of a band of Q1D electrons due to spatial perturbations, and its critical role in carrier scattering, have only been studied theoretically.<sup>7-9</sup> Meanwhile, nonlinear screening effects have very recently been investigated in theory and experiments on two-dimensional carriers: in GaAs-AlGaAs quantum wells, by optically probing the low-density (percolation) limit,<sup>13</sup> in graphene with its semimetallic and relativistic dispersion, as an important effect for in-plane charge transport<sup>14</sup> and in-plane PN junctions,<sup>15</sup> and perpendicular to the plane in gated multilayer graphene.<sup>16</sup>

In this work we explicitly study nonlinearity of the dielectric response and scattering of electrons in InAs NWs with diameter down to 28 nm, due to a repulsive Coulomb impurity with charge  $q = -e$ . Fully quantum mechanical carrier dielectric response and scattering theory is compared to experiments determining the conductance  $G_D$ <sup>8</sup> of scattering by single Coulomb impurities, in connection with our previous study of high temperature ultrahigh sensitivity of InAs NW conductance to localized charge.<sup>17</sup> The comparison reveals that  $G_D$  contains valuable information about physical processes governing the many-body dielectric response of carriers in Q1D systems. The scattering embodied by  $G_D$  is enhanced by two orders of magnitude for NWs with diameter  $d \approx 30$  nm by the combination of nonlinear screening and the renormalization of the Coulomb interaction due to dielectric mismatch (DMM). Here DMM refers to the NW's large dielectric permittivity  $\epsilon$  compared to  $\epsilon_{\text{out}}$  of its environment, renormalizing carrier-impurity and carrier-carrier Coulomb interactions.<sup>2,18,19</sup>

The identified nonlinearity in dielectric response is unusually strong, occurring in the presence of just a single electron.

It relies on the renormalization of the Coulomb interaction due to DMM, producing a self-consistent suppression of local density of states and carrier susceptibility at the Fermi energy. Consistent with the NW radius  $R$  being similar to the long-wavelength Thomas-Fermi screening length  $\lambda$ , the effects become stronger with decreasing NW diameter. We also find that repulsively charged impurities scatter carriers like a potential barrier many  $k_B T$  in energy and much more strongly than attractive impurities, explaining how a single Coulomb impurity can control the conductance of a 1  $\mu\text{m}$  long NW<sup>17</sup> even if many attractive Coulomb impurities are present as is typical for InAs NWs.<sup>20</sup> The nonlinear screening and DMM contribute to a nontrivial description of many-body carrier screening in 1D structures that is nevertheless found to be necessary for agreement between theory and experiments for scattering by a lone repulsive impurity in a nanowire.

We obtain  $G_D$  experimentally by gate-voltage ( $V_{GS}$ ) resolved measurements of two conductance levels corresponding to repulsive and neutral charge states of an impurity observed in two-level random telegraph noise (RTN)<sup>21</sup> in InAs NWs. We validate our theory of dielectric response including the nonlinearity and DMM for NWs covering a range of diameters  $d \approx 30$ –60 nm.

The treatment of nonlinear screening clarifies the properties of NWs in an important regime of departure from existing theoretical work on linear scattering and screening<sup>7,9</sup> that will be of particular scientific interest as quasi-one-dimensional properties begin to be realized in these structures<sup>10-12</sup> and as nanowires are used as a platform for realization of Majorana fermions.<sup>22</sup> The results will also find significant practical importance in NW-based sensors,<sup>23</sup> single-electron memories,<sup>24</sup> and transistors,<sup>10</sup> where response of conductance to localized charge determines crucial device performance parameters. In particular, nonlinear screening and dielectric mismatch imbue the ultrahigh charge sensitivity ( $dQ \approx 10 \mu\text{eHz}^{-0.5}$ ) of InAs NWs recently reported by the authors.<sup>17</sup>

Single-crystal wurtzite InAs NWs for the study were grown by molecular beam epitaxy (MBE) and transferred to  $p^{++}$  Si wafers coated with 100 nm of SiO<sub>2</sub>. Metallic

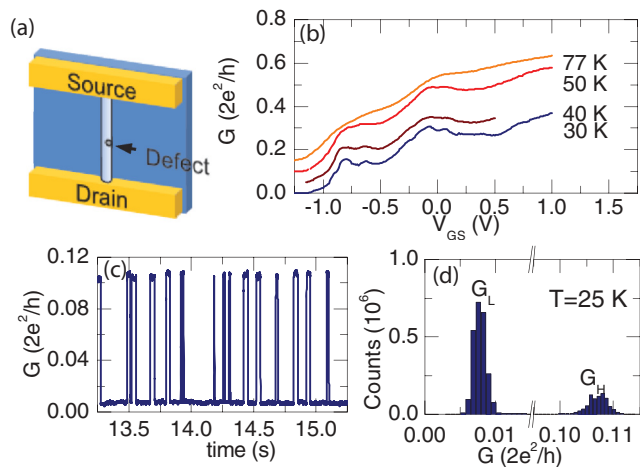


FIG. 1. (Color online) (a) Schematic of contacted NW. (b)  $G$  vs  $V_{GS}$  for NW1 at  $T = 30, 40, 50,$  and  $77$  K, offset by  $0.05(2e^2/h)$ , for clarity. (c) RTN of NW2 at  $T = 25$  K and  $V_{GS} - V_T = 0.115$  V, with  $V_T$  defined for the neutral trap state, that is,  $G_H(V_{GS})$  in Fig. 2(a). (d) Distribution of conductance for RTN in (c).

Ti(10 nm)/Au(100 nm) electrodes spaced  $L = 1000$  nm apart were patterned by electron beam lithography. Details are given elsewhere.<sup>17</sup> Resulting devices are schematically illustrated in Fig. 1(a). Wire-bonded chip carriers containing diced chips were loaded into a variable temperature helium cryostat and pumped for typically 24 h using a turbomolecular pump prior to electrical measurements. After pumping, the conductance of  $\approx 30$  nm diameter NWs is typically an order of magnitude more than those in air.

The dependence of the differential conductance  $G = I_{DS}/V_{DS}$  on  $V_{GS}$  applied to the  $p++$  substrate, measured using a lock-in with  $V_{DS} < k_B T$ , is shown for NW1 with  $d = 34 \pm 2$  nm in Fig. 1(b). Here  $V_{DS}$  and  $I_{DS}$  are the bias across and current flowing through the NW, respectively. The peak field-effect mobility of electrons estimated using the charge control model<sup>25</sup> is  $\mu_{FE} \approx 23\,000$  cm<sup>2</sup> V<sup>-1</sup> s<sup>-1</sup> at  $T = 30$  K. Out of 34 InAs NWs screened, nine we found to exhibit RTN, stochastic capture, and emission of an electron from a single trap on the NW's surface. A typical RTN is shown in Fig. 1(c) for NW2 with  $d = 28 \pm 2$  nm and  $\mu_{FE}$  similar to that of NW1. The trapping cross section and dependence of trap energy on gate voltage, discussed in detail elsewhere,<sup>20</sup> support assignment of the position of the active trap to the interface between the InAs NW and its 2–3 nm oxide. We observed similar RTN in NWs suspended over trenches.

The distribution of conductances within two-level RTN is characterized by two peaks centered at  $G_H$  and  $G_L$  as shown in Fig. 1(d). With increasing  $V_{GS}$ , the low conductance is increasingly statistically favored, from which we conclude that it is produced by charging the defect with an additional electron.<sup>20</sup> The dependence of  $G_H$  and  $G_L$  on  $V_{GS}$  is shown in Fig. 2(a) for NW2 ( $d = 28 \pm 2$  nm) at  $T = 25$  K and NW3 ( $d = 59 \pm 2$  nm) at  $T = 34$  K. The single impurity conductance<sup>8</sup>  $G_D = (G_L^{-1} - G_H^{-1})^{-1}$ , expected to have little or no contribution from phase coherent effects at this temperature,<sup>26</sup> depends exponentially on  $V_{GS}$  as shown in Fig. 2(b). Therefore we conclude that carrier scattering is dominated by thermionic emission over a repulsive Coulomb

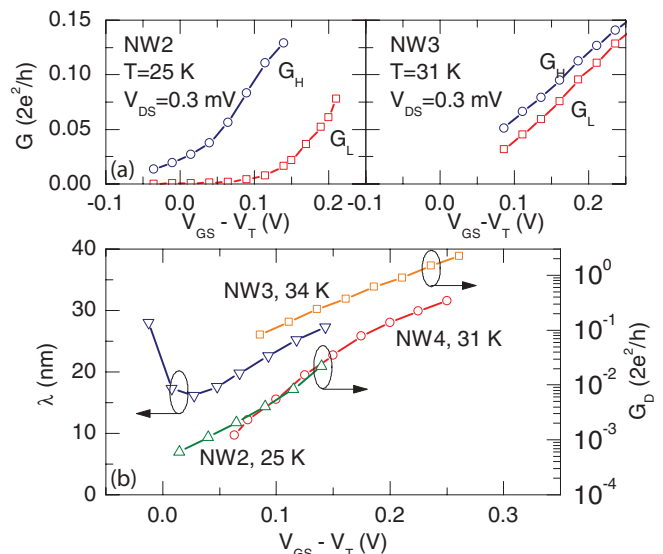


FIG. 2. (Color online) (a)  $G_H$  (open circles) and  $G_L$  (open squares) vs  $V_{GS}$  for NW2 at  $T = 25$  K, NW3 at  $T = 34$  K. (b)  $G_D$  vs  $V_{GS}$  for NW2, NW3, and NW4 ( $d = 33 \pm 2$  nm,  $T = 31$  K) and TF screening length  $\lambda$  estimated from carrier density  $n$ . A subset of the data is also shown in Ref 17.

barrier several  $k_B T$  in energy. Results for NW4 ( $d = 33 \pm 2$ ) at  $T = 31$  K, shown in Fig. 2(b), are in close agreement with NW2, but  $G_D$  is much less for NW2 and NW4 compared to NW3, whose diameter is twice as large. The carrier scattering probability,  $1 - G_D/G_0$ , where  $G_0 = 2e^2/h$ , is 0.999–0.900 for  $0.00$  V  $< V_{GS} - V_T < 0.20$  V.

The following considerations reveal that electronic subband quantization effects may be expected in carrier scattering processes in our experiments. Taking nonparabolicity of the conduction band into account, the estimated energy of electronic subband quantization between the second and first subbands is  $E_2 - E_1 \approx 50$  meV  $\gg k_B T$  due to geometrical confinement of electrons in a 30 nm diameter cylindrical hard-wall InAs NW.<sup>17,27</sup> Moreover, the carrier density  $n = C(V_{GS} - V_T)/e\pi R^2 L$ , where  $C$  is the gate capacitance, satisfies  $n < 20$   $\mu\text{m}^{-1}$  for  $V_{GS} - V_T < 0.2$  V, much less than the carrier density  $\approx 130$   $\mu\text{m}^{-1}$  at the onset of filling the second subband. Even in nonballistic NWs with relatively more disorder than is evident from  $\mu_{FE}$  of our NWs, subband electronic structure is expected to emerge in  $G$  vs  $V_{GS}$ .<sup>4</sup> The plateau structure seen in Fig. 1(b) is frequently observed in our MBE grown NWs, with  $V_{GS}$  at successive plateaus consistent with subband electronic structure expected as above. Finally, we can expect DMM to be important for carrier dielectric response since the TF screening length of Q1D carriers,<sup>5</sup> estimated from  $n$  and temperature  $T$  and shown in Fig. 2(b), is similar to  $R$ .

We now investigate the role of DMM, the linearity of carrier dielectric response, and their influence on both  $G_D$  and threshold voltage  $\Delta V_T$  shift apparent between  $G_H$  and  $G_L$ . Carrier dielectric response, which determines both the single impurity scattering potential and therefore  $G_D$  and  $\Delta V_T$ , is considered within a fully microscopic quantum-mechanical context employing the effective mass approximation. Intermediate results are presented for the special case of  $R = 15$  nm,

but excellent agreement between theory and experiments is obtained for the full range of NW diameters 30–60 nm in experiments as shown in Fig. 4. In our previous work on charge sensitivity of InAs NWs,<sup>17</sup> the comparison with theory employed a simplified semiclassical (long-wavelength) analysis of screening, combined with phenomenological carrier transport. This approach has the well-known deficiency that the kinetic energy and therefore short-wavelength behavior is not accurately represented. The success of the fully microscopic approach herein underscores the importance of short wavelength behavior in describing the dielectric response of 1D systems in particular for electron scattering by impurities.

An unscreened Coulomb impurity with charge  $q = -e$  at  $\mathbf{r} = \mathbf{r}_0$  produces a potential  $U_a(\mathbf{r})$  from which we define an effective one-dimensional potential  $U_a(z) = \int r dr d\theta |\varphi_1(r, \theta)|^2 U_a(\mathbf{r})$ . We assume a cylindrically symmetric subband electron density  $|\varphi_1(r, \theta)|^2$ .<sup>28</sup> Taking DMM into account in  $U_a(\mathbf{r})$ <sup>19</sup> via an effective outer dielectric  $\epsilon_{\text{out}} = 1.6\epsilon_0$  determined by three-dimensional finite element calculations, and assuming a radial hard-wall confinement,<sup>27</sup> we obtain  $U_a(z)$  in Fig. 3(a) peaking at  $\approx 38$  meV vs  $\approx 9$  meV when  $\epsilon_{\text{out}} = 15\epsilon_0$ .

The single defect conductance  $G_D = 2e^2/h \int dE T(E) (-\partial f/\partial E)$ ,<sup>8</sup> where  $f(E)$  is the Fermi-Dirac distribution, depends on the transmission probability  $T(E)$

for scattering by a self-consistent, carrier-screened potential  $U(z)$ . We solve  $U(z)$  by two different methods: self-consistent linear mean-field screening and exact (nonlinear) mean-field screening. Transmission  $T(E)$  is obtained by solving an effective 1D Schrödinger equation  $[-(\hbar^2/2m)d^2/dz^2 + U(z)]\phi_{E(k)}(z) = [E(k) - E_1]\phi_{E(k)}(z)$  for electronic envelope functions  $\phi_{E(k)}(z)$  and energies  $E(k) - E_1$ , where  $E_1$  is the conduction band edge, using open boundary conditions.<sup>29</sup> In linear screening the electron density is perturbed to first order by the self-consistent potential  $U(z) = U_a(z) + U_s(z)$  whose Fourier components are  $U(q) = U_a(q)/\epsilon(q)$ , where  $U_a(q)$  are Fourier components of  $U_a(z)$ ,  $\epsilon(q) = 1 - F(q, E_F, T)U_{1,1}(q)$  is the dielectric response,  $F(q, E_F, T)$  is the Lindhard function,  $E_F$  is the Fermi energy,  $U_{1,1}(q) = \int r dr d\theta |\varphi_1(r)|^2 U_{1,1}(r, q)$  is the unscreened interaction,<sup>1,3</sup> and  $U_{1,1}(r, q)$  satisfies the Poisson equation

$$\left[ \frac{1}{r} \frac{d}{dr} \epsilon(r) r \frac{d}{dr} - \epsilon(r) q^2 \right] U_{1,1}(r, q) = -e^2 \frac{|\varphi_1(r)|^2}{l}. \quad (1)$$

Here  $\epsilon(r) = \epsilon$  for  $r < R$  and  $\epsilon(r) = \epsilon_{\text{out}}$  for  $r \geq R$ , and  $l$  is an artificial periodicity.

The nonlinear screening process considered takes into account how screening is modified by the self-consistent change in local density of states in the NW. Poisson and Schrödinger equations were solved self-consistently using an approximate Jacobian,<sup>30</sup> taking the electron density as  $n[U(z)] = 2 \sum_k f[E(k), E_F, T] |\phi_{E(k)}(z)|^2$ . We investigate the influence exchange on scattering by augmenting  $U(z)$  in the Schrödinger equation with an exchange potential in the local density approximation (LDA),  $U_x(z) = \int r dr d\theta |\varphi_1(r, \theta)|^2 U_x(\mathbf{r})$ ,  $U_x(\mathbf{r}) = -e^2 [3\pi^2 n(\mathbf{r})]^{1/3} / 4\pi^2 \epsilon$ .<sup>31</sup>

Results for  $U(z)$  and  $n(z)$  in both approaches are shown in Figs. 3(b) and 3(c), respectively, for  $n = 10 \mu\text{m}^{-1}$  (left) and  $n = 20 \mu\text{m}^{-1}$  (right), at  $T = 30$  K. For  $n = 10 \mu\text{m}^{-1}$ , the electron density  $n(z) = \int dz' K(z - z') U_s(z') + n$ , where  $K(z) = \sum_q \exp(iqz) / [U_{1,1}(q)l]$ , predicted by linear screening drops well below zero indicating an internal inconsistency in linear response. Nonlinear screening remedies the problem by correctly reducing the susceptibility and therefore dielectric response in the region where local density of states is suppressed. As a result, the Coulomb scattering barrier [Fig. 3(c)] is stronger, peaking at  $\approx 17$  meV, 70% larger than the barrier  $\approx 10$  meV predicted by linear screening. The exchange potential introduces a modest  $\approx 1$  meV contribution to  $U(z)$ . For  $n = 20 \mu\text{m}^{-1}$  there is still a noticeable difference between the linear and nonlinear screening, and for larger electron densities, the discrepancy decreases. Crucially, similar analysis for  $\epsilon_{\text{in}} = \epsilon_{\text{out}} = 15\epsilon_0$  reveals the screening is essentially linear (dotted lines) for both  $n = 10 \mu\text{m}^{-1}$  and  $n = 20 \mu\text{m}^{-1}$  for  $R = 15$  nm. Quantities  $U(z)$  and  $U_a(z)$  were found to be practically independent of  $|\varphi_1(r, \theta)|^2$ .

Calculated electron reflection spectra  $R(E) = 1 - T(E)$  for nonlinear screened potentials are shown in Fig. 4(a) for  $n = 10 \mu\text{m}^{-1}$  (left) and  $n = 20 \mu\text{m}^{-1}$  (right) at  $T = 30$  K. Attractive impurities (dashed) weakly scatter carriers ( $R < 0.01$ ,  $n = 10 \mu\text{m}^{-1}$ ), compared to repulsive impurities (solid) ( $R \approx 0.99$  same  $n$ ), though the disparity decreases with increasing  $n$ . Considering  $E_F$  and  $k_B T$  scales in Fig. 4(a),

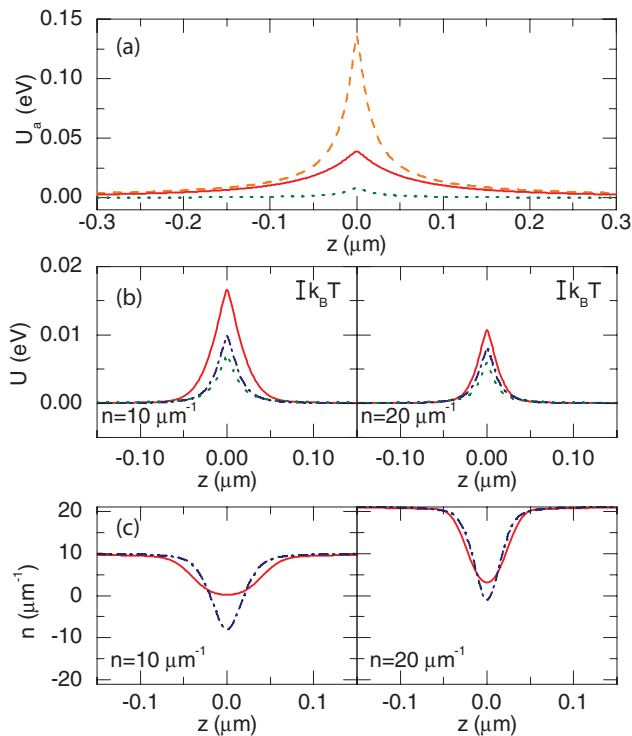


FIG. 3. (Color online) For  $d = 30$  nm InAs NW. (a) Calculated  $U_a(z)$  for impurity 2 nm into surface of NW with  $[\epsilon, \epsilon_{\text{out}}] = [15\epsilon_0, 1.6\epsilon_0]$  (solid),  $[\epsilon, \epsilon_{\text{out}}] = [\epsilon_0, \epsilon_0]$  (dashed),  $[\epsilon, \epsilon_{\text{out}}] = [15\epsilon_0, 15\epsilon_0]$  (dotted). Calculated (b)  $U(z)$  and (c)  $n(z)$  for  $n = 10 \mu\text{m}^{-1}$  (left) and  $n = 20 \mu\text{m}^{-1}$  (right) using nonlinear (line) and linear (dash-dot) screening with  $[\epsilon, \epsilon_{\text{out}}] = [15\epsilon_0, 1.6\epsilon_0]$ , and nonlinear screening with  $[\epsilon, \epsilon_{\text{out}}] = [15\epsilon_0, 15\epsilon_0]$  at  $T = 30$  K [dotted, only in (b)].

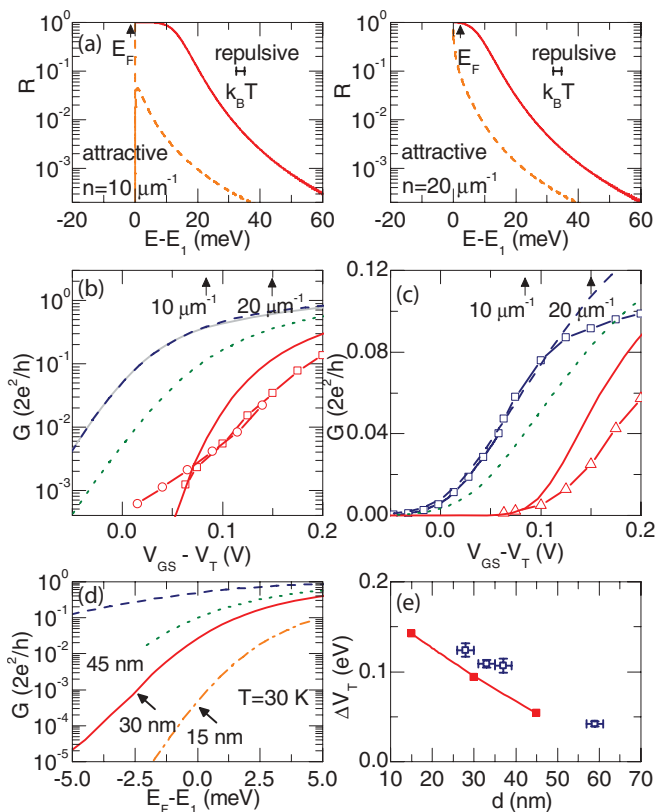


FIG. 4. (Color online) (a)  $R(E)$  for nonlinear screened repulsive (solid) and attractive (dashed) Coulomb impurities for  $n = 10 \mu\text{m}^{-1}$  (left) and  $n = 20 \mu\text{m}^{-1}$  (right) at  $T = 30$  K. (b) Single defect conductance  $G_D$  and (c)  $G_H$  and  $G_L$  for repulsive Coulomb impurity. Data (open symbols) are connected by solid lines. Theory has  $[\epsilon, \epsilon_{\text{out}}] = [15\epsilon_0, 1.6\epsilon_0]$  (solid),  $[\epsilon, \epsilon_{\text{out}}] = [15\epsilon_0, 15\epsilon_0]$  (dotted), and for (b) scattering by an attractive Coulomb impurity  $[\epsilon, \epsilon_{\text{out}}] = [15\epsilon_0, 1.6\epsilon_0]$  (solid gray) is included for reference (dashed), along with  $T(E) = 1$  (dashed). (d) Dependence of single defect conductance on gate voltage for different NW diameters at  $T = 30$  K. (e)  $\Delta V_T$  vs NW diameter for experiments (open) and theory (solid),  $T = 30$ – $50$  K.

we remark that only the repulsive impurity produces the signature of thermionic emission in  $G_D(V_{GS})$ . Calculated  $G_D$  considering nonlinear screening, shown in Fig. 4(b), can be suppressed by nearly two orders of magnitude when DMM (solid) is taken into account, compared with  $\epsilon_{\text{out}} = 15\epsilon_0$  (dotted). In comparison,  $G_D$  for an attractive defect (solid) nearly overlaps the case  $T(E) = 1$  (dashed) shown for reference. Calculated  $G_D$  considering nonlinear screening is within a factor of 2 of measured data (open points), a disparity  $k_B T \log(2) \approx 1.8$  meV in effective barrier height between theory and experiments.

Choosing  $T(E_F) \sim \text{const}$  reproduces  $G_H(V_{GS})$  permitting comparison of  $G_L$  between theory (lines) and experiments (open points) in Fig. 4(c). Excellent agreement is obtained only if DMM and nonlinear screening is included in the model (solid lines). Ignoring DMM, calculated  $G_D$  (dashed) lacks the threshold voltage shift  $\Delta V_T$  apparent in data. For NW4, measured  $\Delta V_T = 109 \pm 5$  mV is in close agreement with  $\Delta V_T = 94 \pm 1$  mV predicted considering nonlinear dielectric response. In comparison, a semiclassical/phenomenological

drift/diffusion description<sup>17</sup> which only captures the  $q \rightarrow 0$  behavior is in considerable error with these calculations and measurements.

The mapping between  $V_{GS}$  and  $E_F - E_1$ , required for Figs. 4(b), 4(c), and 4(e), is provided by an electrostatic model with a cylindrical NW, planar backgate, and a surface state density  $D_{ss} = 2 \times 10^{12} \text{ cm}^{-2} \text{ eV}^{-1}$  deduced from the subthreshold characteristics and supported by independent analysis of RTN dynamics presented elsewhere.<sup>20</sup> Calculations for different NW diameters reveal that scattering rate [Fig. 4(d)] and nonlinearity of dielectric response both increase in strength with decreasing diameter for fixed  $n$ . Evidently from Fig. 4(e), measured (open points) and calculated (solid line)  $\Delta V_T$  agree for representative NWs of different diameter down to  $d = 30$  nm and temperatures in the range  $T = 30$ – $50$  K. Based on analysis of measured random telegraph signals at different temperatures,  $\Delta V_T$  appears relatively unchanged with temperature up to at least 200 K.

Unlike the small and diameter-independent exchange correction, DMM-mediated enhancement to the Coulomb scattering barrier—including the effect of nonlinear screening encapsulated in  $\epsilon(q)$ —becomes increasingly important with decreasing diameter. The Coulomb barrier  $U(z) = \sum_q U_a(q)/\epsilon(q) \exp(iqz)$  is influenced directly by DMM through the strong enhancement of the bare Coulomb potential  $U_a(z)$  exhibited in Fig. 3(a), and indirectly through the nonlinearity in dielectric response. This nonlinearity is traced back to the self-consistent polarizability  $\chi(q) \sim F(q, E_F, T)$  of the electron gas. Whereas the recently predicted nonlinear, minority carrier screening in multilayer graphene is purely an effect of electronic structure,<sup>16</sup> in the present case, the nonlinearity is only appreciable in the presence of DMM for NW diameters considered. Onset of the predicted nonlinearity occurs for just a single charge and carrier densities of intermediate degeneracy [see  $E_F$  in Fig. 4(a)], though it could also be present at higher densities and larger perturbations such as might be expected in plasma oscillations, or for large fields required for dielectrophoresis of NWs.<sup>32</sup>

The prediction that attractive impurities scatter weakly compared to repulsive impurities [Figs. 4(a) and 4(b)] was obtained elsewhere,<sup>6</sup> but experimental evidence is elusive as the number and nature of impurities is generally not known, although ionized impurities producing the majority carriers are attractive by definition. The presence of attractive defects is guaranteed in our NWs, producing conduction at  $V_{GS} = 0$ . We point out that only the repulsive Coulomb defect can be responsible for the “giant” RTN in Fig. 1(b). The asymmetry also explains the crucial point of how a single Coulomb impurity consistently controls the conductance of a NW provided, as verified by occupation statistics, it is repulsive. Owing to the relatively weak scattering of carriers by attractive impurities, their presence is also not inconsistent with  $G$  vs  $V_{GS}$  exhibiting steps in NWs as long as  $1 \mu\text{m}$ , as shown in Fig. 1(b), clarifying an important aspect of electronic transport in NWs that so far has not been commented on. At higher electron densities where screening is more efficient, the nonlinearity, disparity between attractive and repulsive Coulomb scattering, and their overall scattering strength is reduced.

In conclusion, we measured the single-impurity scattering conductance<sup>8</sup> and show by comparison with theory that it is

a valuable tool for probing the dielectric response of Q1D carriers. For electron densities where TF screening length is similar to NW radius, we find a nonlinear screening process, where suppression of local density of states in the vicinity of the impurity weakens screening. It is essential for obtaining quantitative agreement between experiments and theory. Estimates for carrier scattering by repulsive impurities ignoring DMM and nonlinear response underestimate the Coulomb interaction and scattering probability of carriers by repulsive impurities by 1–2 orders of magnitude. Decreasing NW radius enhances both the nonlinearity and scattering rate. Scattering by attractive impurities, producing majority carriers

in our InAs NWs, is found to be extremely weak in comparison, explaining how a single impurity can control NW conductance, as observed in experiments. The strong connection between weakened screening and scattering in NWs is likely to be of use in technological applications such as NW-based sensors, memories, and transistors where useful signal derives from scattering of electrons by nearby localized charge.

The authors would like to thank A. Shik and G. Tettamanzi for valuable discussions and feedback on the manuscript, and NSERC, CSA, CIPI, OCF, and OCE programs for financial support.

\*joseph.salfi@utoronto.ca

- <sup>1</sup>J. Lee and H. N. Spector, *J. Appl. Phys.* **57**, 366 (1985).
- <sup>2</sup>A. Shik, *J. Appl. Phys.* **74**, 2951 (1993).
- <sup>3</sup>S. Das Sarma and W.-Y. Lai, *Phys. Rev. B* **32**, 1401 (1985).
- <sup>4</sup>S. Das Sarma and X. C. Xie, *Phys. Rev. B* **35**, 9875 (1987).
- <sup>5</sup>J. A. Reyes and M. del Castillo-Mussot, *Phys. Rev. B* **57**, 9869 (1998).
- <sup>6</sup>M. Moško and P. Vagner, *Phys. Rev. B* **59**, R10445 (1999).
- <sup>7</sup>D. Jena and A. Konar, *Phys. Rev. Lett.* **98**, 136805 (2007).
- <sup>8</sup>M. Persson, H. Mera, Y.-M. Niquet, C. Delerue, and M. Diarra, *Phys. Rev. B* **82**, 115318 (2010).
- <sup>9</sup>A. Konar, T. Fang, and D. Jena, *Phys. Rev. B* **84**, 085422 (2011).
- <sup>10</sup>J. Xiang, W. Lu, Y. Hu, Y. Wu, H. Yan, and C. M. Lieber, *Nature (London)* **441**, 489 (2006).
- <sup>11</sup>A. V. Kretinin, R. Popovitz-Biro, D. Mahalu, and H. Shtrikman, *Nano Lett.* **10**, 3439 (2010).
- <sup>12</sup>A. C. Ford, S. B. Kumar, R. Kapadia, J. Guo, and A. Javey, *Nano Lett.* **12**, 1340 (2012).
- <sup>13</sup>M. Yamaguchi, S. Nomura, T. Maruyama, S. Miyashita, Y. Hirayama, H. Tamura, and T. Akazaki, *Phys. Rev. Lett.* **101**, 207401 (2008).
- <sup>14</sup>M. I. Katsnelson, *Phys. Rev. B* **74**, 201401(R) (2006).
- <sup>15</sup>L. M. Zhang and M. M. Fogler, *Phys. Rev. Lett.* **100**, 116804 (2008).
- <sup>16</sup>M. Kuroda, J. Tersoff, and G. Martyna, *Phys. Rev. Lett.* **106**, 116804 (2011).
- <sup>17</sup>J. Salfi, I. G. Savelyev, M. Blumin, S. V. Nair, and H. E. Ruda, *Nat. Nanotech.* **5**, 737 (2010).
- <sup>18</sup>L. V. Keldysh, *Phys. Status Solidi A* **164**, 3 (1997).
- <sup>19</sup>E. A. Muljarov, E. A. Zhukov, V. S. Dneprovskii, and Y. Masumoto, *Phys. Rev. B* **62**, 7420 (2000).
- <sup>20</sup>J. Salfi, N. Paradiso, S. Roddaro, S. Heun, S. V. Nair, I. G. Savelyev, M. Blumin, F. Beltram, and H. E. Ruda, *ACS Nano* **5**, 2191 (2011).
- <sup>21</sup>K. S. Ralls, W. J. Skocpol, L. D. Jackel, R. E. Howard, L. A. Fetter, R. W. Epworth, and D. M. Tennant, *Phys. Rev. Lett.* **52**, 228 (1984).
- <sup>22</sup>V. Mourik, K. Zuo, S. M. Frolov, S. R. Plissard, E. P. A. M. Bakkers, and L. P. Kouwenhoven, *Science* **336**, 1003 (2012).
- <sup>23</sup>N. S. Ramgir, Y. Yang, and M. Zacharias, *Small* **6**, 1705 (2010).
- <sup>24</sup>L. Guo, E. Leobandung, and S. Y. Chou, *Science* **275**, 649 (1997).
- <sup>25</sup>A. C. Ford, J. C. Ho, Y.-L. Chueh, Y.-C. Tseng, Z. Fan, J. Guo, J. Bokor, and A. Javey, *Nano Lett.* **9**, 360 (2009).
- <sup>26</sup>A. Hansen, M. Björk, C. Fasth, C. Thelander, and L. Samuelson, *Phys. Rev. B* **71**, 205328 (2005).
- <sup>27</sup>S. Roddaro, A. Pescaglioni, D. Ercolani, L. Sorba, and F. Beltram, *Nano Lett.* **11**, 1695 (2011).
- <sup>28</sup>This can be justified for nanowires with small enough diameters and electron densities that the subband quantization, including the constant offset potential of cylindrically symmetric surface doping but ignoring free electron potential, exceeds the electrostatic potential  $-e\Phi(r)$  induced by the free electron density.
- <sup>29</sup>C. S. Lent and D. J. Kirkner, *J. Appl. Phys.* **67**, 6353 (1990).
- <sup>30</sup>D. Vasileska, D. Mamaluy, H. R. Khan, K. Raleva, and S. M. Goodnick, *J. Comput. Theor. Nanosci.* **5**, 999 (2008).
- <sup>31</sup>C. Delerue and M. Lannoo, *Nanostructures, Theory and Modeling* (Springer, Berlin, 2004).
- <sup>32</sup>H. E. Ruda and A. Shik, *J. Appl. Phys.* **109**, 064305 (2011).